Multi-modal sensing in spin crossover compounds — **Source link** ↗

Denis Gentili, Nicola Demitri, Bernhard Schäfer, Fabiola Liscio ...+5 more authors

Institutions: Elettra Sincrotrone Trieste, Karlsruhe Institute of Technology, University of Strasbourg
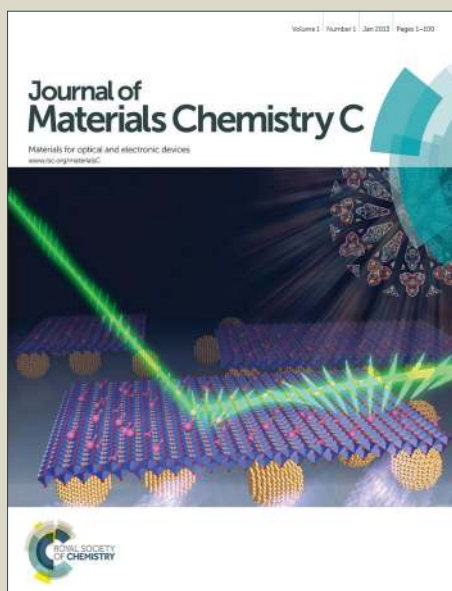
Related papers:

- Molecular spin crossover phenomenon: recent achievements and prospects

- Three-Way Crystal-to-Crystal Reversible Transformation and Controlled Spin Switching by a Nonporous Molecular Material

- Spin-Transition Polymers: From Molecular Materials Toward Memory Devices

- Structure:function relationships in molecular spin-crossover complexes

- Spin state switching in iron coordination compounds

Multi-modal sensing in spin crossover compounds

Denis Gentili[1,a], Nicola Demitri[2,a], Bernhard Schäfer [3], Fabiola Liscio[4], Ilaria Bergenti[1], Giampiero Ruani[1], Mario Ruben[3,5] and *Massimiliano Cavallini*[1,6]

1) Istituto per lo Studio dei Materiali Nanostrutturati-Consiglio Nazionale delle Ricerche, Via P. Gobetti 101, 40129 Bologna (Italy)

2) Elettra - Sincrotrone Trieste, S.S. 14 Km 163.5 in Area Science Park, 34149 Basovizza – Trieste (Italy).

3) Institute of Nanotechnology, Karlsruhe Institute of Technology, D-76344 Eggenstein-Leopoldshafen (Germany).

4) Istituto per la Microelettronica e i Microsistemi -Consiglio Nazionale delle Ricerche-Via P. Gobetti 101, 40129 Bologna

5) Institut de 6Physique et Chimie des Matériaux de Strasbourg (IPCMS), CNRS-Université de Strasbourg, 23, rue du Loess, BP 43, 67034, Strasbourg cedex 2 (France).

6) Scriba Nanotechnologie S.r.l. Via di Corticella 183/8 40128 Bologna, (Italy).

E-mail: massimiliano.cavallini@cnr.it

Note: a) DG and ND contributed in the same manner to this manuscript.

1

Abstract

We exploited the solvatochromic spin-state switching in a spin crossover (SCO) compound based on Fe^{II} complex and the simultaneous change of spectroscopic properties for selective multimodal sensing to methanol and ethanol. We demonstrate that sensing capabilities is due to the inclusion of methanol or ethanol molecules into the crystalline structure, which tailor simultaneously the transition temperature, colour, birefringence and vibrational modes. We exploited this capability by integrating a neutral compound, switchable at room temperature, in a micrometric TAG sensible to the colour and birefringence.   The system were characterised by optical microscopy, magnetic susceptibility, Raman spectroscopy and X-ray diffraction.

D. Gentili et al. *J. Mater. Chem. C*

1. Introduction

Spin crossover (SCO) compounds are transition metal complexes capable to switch their spin state upon external stimuli such as temperature, pressure, magnetic field and light[1]. Typically they are formed by a transition metal with $3d^4$-$3d^7$ configurations, in which the "d electrons" can be distributed, paired or unpaired, depending on the difference of energy between t_{2g} and e_g^* d-orbitals. The switching involves a structural transition that produces a change of d-orbital splitting and consequently the electron redistribution (*viz.* the spin transition), as well the change of many physical properties such as: colour, magnetic susceptibility, thermal/electric conductivity, dielectric constant, diffraction and mechanical properties[2-7]. Key parameters for the useful use of SCO are the transition temperature and the processability, in this respect compounds with transition temperature close to room temperature and suitable for surface deposition are highly desirable[8-10]. SCO phenomenon depends on the molecular packing, crystallinity, anions and eventually from solvent molecules that are often included in the crystal structure[11]. The strong influence of these parameters on SCO properties has been largely investigated and summarised in exhaustive reviews[3, 12-16]. SCO properties can be tailored acting on chemical design of ligands, on nature and size of counter ions and on solvent nature[13, 17, 18], small change of one of this parameters can produce a dramatic change in transition temperature and associated properties[19].

Thanks to their versatility and multifunctional properties, SCO were proposed for many technological applications, such as molecular memories[1, 20-22], chemical[16, 23]/pressure[24] sensors, and organic electronics[25], among them their use as gas/solvent sensors is probably the most advanced application as recently proposed by Bousseksou's group in a sensor device based on micro patterned gratings a SCO molecular organic frameworks[26].

Thanks to the variety of properties associated to the spin transition and their different response to external stimuli, SCO compounds offer a unique opportunity for multi-modal

Journal of Materials Chemistry C **Page 4 of 26**

D. Gentili et al. *J. Mater. Chem. C*

sensing (*i.e.* the sensing capability obtained by more than one measurable physical parameter). Here we report on a study of multi-modal sensing capability of neutral SCO used as selective sensor for methanol and ethanol. We demonstrate that sensing capabilities of a SCO compound are due to the inclusion of alcohol molecules into the crystalline structure of the compound, which tailor the transition temperature and all the associated physical properties. We exploited this capability by integrating a SCO compound in a micrometric TAG sensible to the change of colour, birefringence and Raman properties.

For our purposes we used SCO complex **1**, with molecular formula $[Fe(L)_2]$ (LH: (2-(pyrazol-1-yl)-6-(1H-tetrazol-5-yl)pyridine) (see the chemical structure in the inset of Figure 1), which is a neutral compound switchable around room temperature whose synthesis and characterization is reported elsewhere[27]. As SCO, complexes containing Fe^{II} as metal ions, **1** is particularly interesting since it can exist in diamagnetic state with all electrons paired in t_{2g} orbitals (low spin state, LS) as well as in paramagnetic state, with four electron unpaired distributed between t_{2g} and e_g^* orbitals (high spin state, HS).

2. Results and discussion

2.1 Compound characterization

Complex **1** is a neutral material that crystallizes forming block shaped crystals whose unit cell contains eight complex units $[Fe(L)_2]$ and ten molecules of methanol[27]. Crystals grown from CH_2Cl_2/CH_3OH solution are yellow in the mother liquor and turn red after the evaporation of the surrounding solvents. Figure 1 shows the magnetic characterization of the crystalline powder of **1**, which exhibits a transition temperature centred at 295 K with a hysteresis of ~5 K that appears after the first thermal cycle.
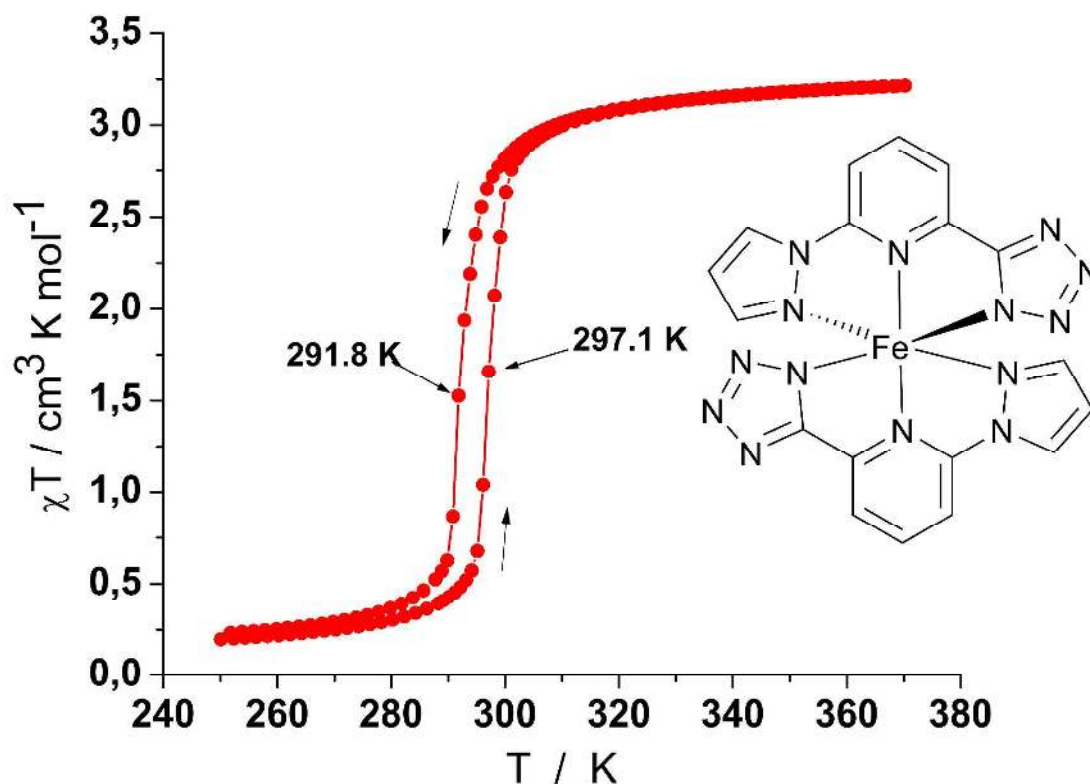
Figure 1 Magnetic characterization and structural formula of compound **1.**

The spin transition can be followed by polarised optical microscopy (OM) and by Raman spectroscopy. Below the transition temperature the powder of **1** is formed by red crystals of a size ranging from a few up to 100 μm. Upon heating up to 300 K, the spin state of the powder crosses over from LS to HS accompanied by a colour change from red to yellow/orange[28]. The transition is associated with a fragmentation of the crystals, probably due to differences in the crystal structures of low and high spin state. Figure 2 shows the colour and birefringence evolution of the SCO crystallites upon thermal cycle. Noticeably, when observed by OM with crossed polars, crystallites in LS state appear almost dark (i.e. do not show birefringence) while crystallites in HS state appear strongly coloured (i.e. show birefringence). Cooling down

the sample below the transition temperature the (fragmented) crystals return to red colour

and lose the birefringence.
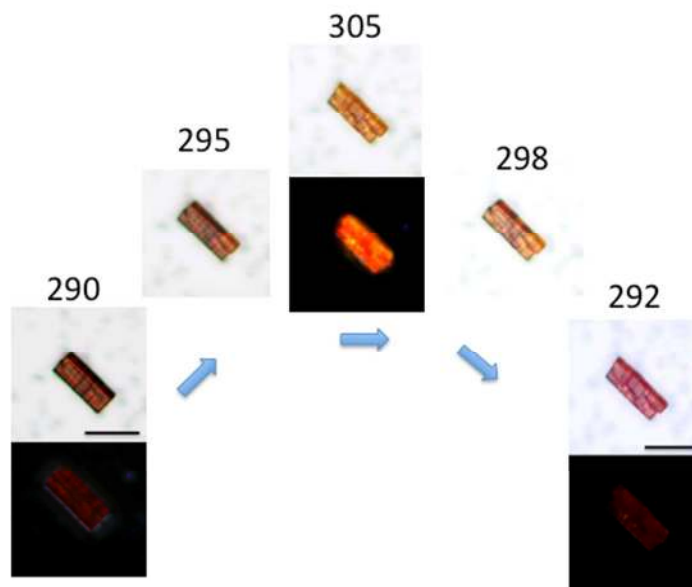

Figure 2. Real time optical and cross-polarised imaging of the SCO crystallites deposited on silicon upon a thermal cycle 290 K→305 K→292 K. Bar is 30 µm. In cross-polarised images, polarizers are oriented parallel and perpendicular to the image axis.

The spin transition of **1** was investigated by µ-Raman spectroscopy, which has been

recognized to be an efficient technique for detecting the spin state in SCO compounds[29].

The use of µ-Raman, with a small laser spot size (<1.5 µm), allows us the detection of the

spectra with the resolution of a single crystallite.

According to magnetic and OM characterization, Raman spectra were collected at different

temperatures, i.e. at 280 K, corresponding to complete transformation of **1** in LS state, and at

328 K, corresponding to complete transformation in HS state (Figure 1). The experiments

were performed on a single crystal, starting from 294 K then, cooling down to 160 K and

subsequently heating up at 328 K and finally cooling again to 280 K. The Raman spectra are

reversible upon thermal cycling.

The overall Raman spectrum strongly depends on the molecule spin state showing several

distinctive (diagnostic) peaks, mostly concentrated in the range 400-1100 cm^{-1}. Figure 3

D. Gentili et al. *J. Mater. Chem. C*

shows the spectra of a specific crystal in the two spin state LS and HS (at 280 K and 328 K respectively).
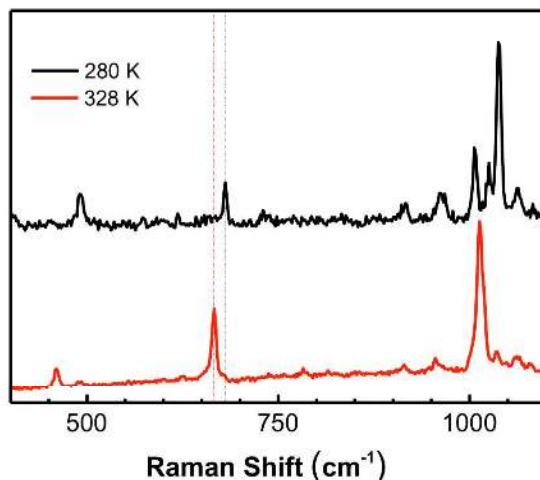
Figure 3. Raman spectra collected at 328K and 280K on a crystallite. The dotted lines indicate the distinctive peak for HS and LS states.

Considering the above data, we concluded that the different spin state of **1** can be directly detected by the colour and/or birefringence and/or Raman spectra, in which the red, poor birefringent state corresponds to the LS state and the yellow (orange), highly birifringent state corresponds to HS state.

2.2 Solvatochromic spin-state-change

Inspired by the fact that the crystals of **1** are in (yellow) HS state in the mother liquor used for their synthesis and turn to (red) LS state after the evaporation of the solvents, we exploited the effect of the switching on several physical properties for multi-modal sensing of methanol and ethanol.

As **1** is exposed to methanol or ethanol at room temperature the crystals turn from red to yellow as in the thermal spin transition. This effect, named solvatochromic spin-state change

7

D. Gentili et al. *J. Mater. Chem. C*

was already observed for several magnetic materials[30], including SCO[19] and is particularly

efficient in neutral compounds[23].

The transition occurs both in vapour atmosphere and in water solution, it occurs in a few

seconds in case of methanol and in a few minutes in the cases of ethanol. Crystals exposed to

methanol switch back to the original red form, in a few seconds, as soon as they are removed

from methanol atmosphere, while crystals exposed to ethanol remain stable in air a few

minutes. No effect was observed by exposing crystallite of **1** to other solvent such as alcohols

bigger than ethanol (probably because the steric hindrance) acetone, dichloromethane, and

chloroform for at the least 30 minutes.

Figure 4 shows the behaviour under polarised OM and Raman spectra recorded at room

temperature of a crystallite in air, and in to methanol (ethanol) saturated atmosphere. It must

be noted that the transition from HS to LS occurs with a mechanism of nucleation and growth

when the crystallites are removed from alcohol atmosphere. The nucleation preferentially

starts at one side of the crystal and propagates to the entire crystal in some ten seconds.

D. Gentili et al. *J. Mater. Chem. C*
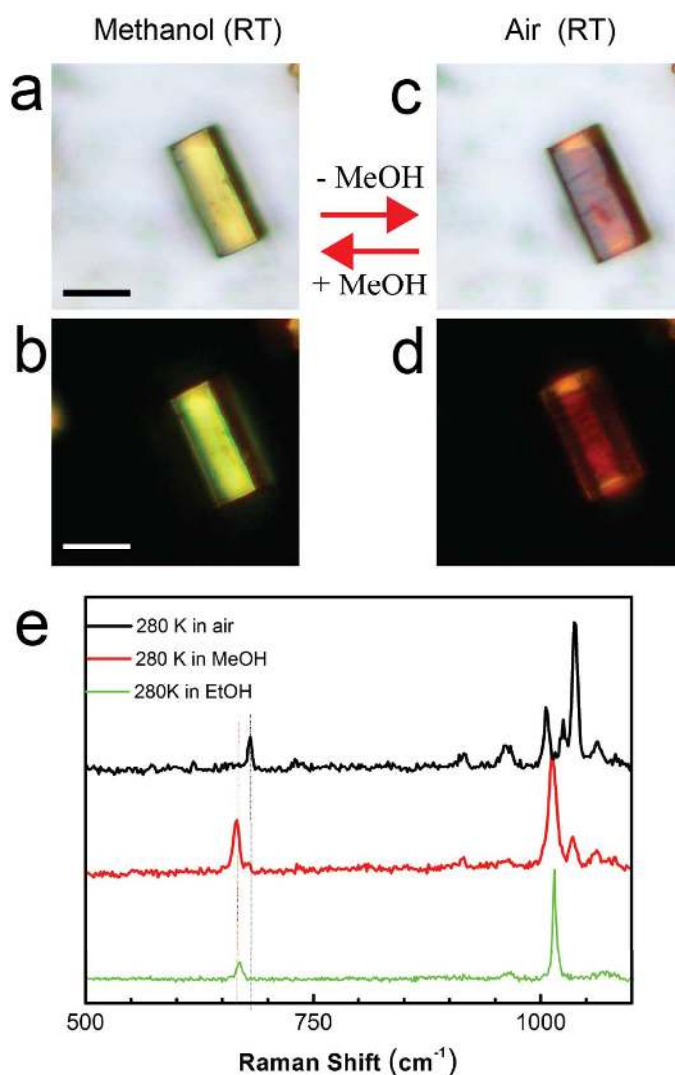
Figure 4. Bright field and cross polarized optical images of a crystallite of **1** recorded at room temperature**.** a, b) Crystal exposed to the methanol (MeOH) vapours at room temperature; c, d) corresponding image of the same crystal in air. e) Comparison between the Raman spectra in air, in methanol and ethanol atmosphere at 280K.

By repeating 10 times the exposition to methanol vapours at room temperature (thus performing the transition from LS to HS and vice versa) no fragmentation was observed. On the other hand, using ethanol, the behaviour of **1,** upon solvent exposure, is more similar to the thermal treatment and crystals tend to fragment after a couple of cycles of solvent exposure. As reported below, this fact can be explained by the different effect of the alcohols on the crystalline structure.

D. Gentili et al. *J. Mater. Chem. C*

Figure 5 shows the thermal behaviour at OM of a crystallite in saturated atmosphere of

ethanol. Interestingly, under these conditions a shift of the spin state transition temperature,

from 294 K to 248 ±3 K (272 ±3 K for methanol) was observed.
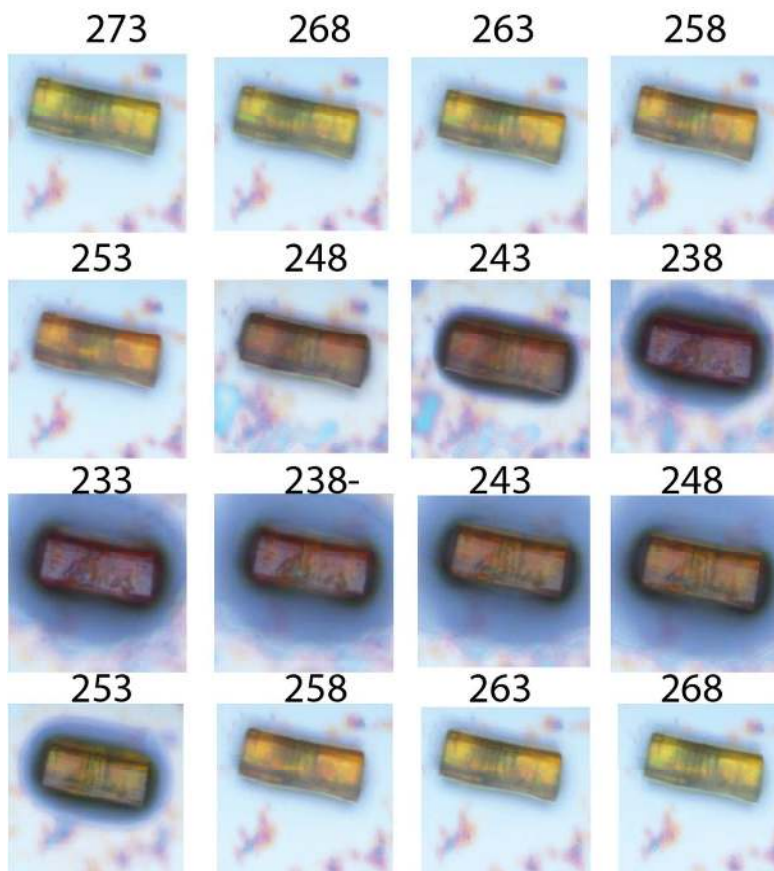
Figure 5. Real time optical imaging of the temperature dependence of the colour of a crystallite of **1** deposited on silicon and recorded in saturated atmosphere of ethanol. The sample was prepared at room temperature in air than it was exposed to ethanol-saturated atmosphere, cooled at 233 K and then heated again at room temperature.

The thermal behaviour of crystallites in methanol-saturated atmosphere was monitored by

Raman spectra. Figure 6 shows the evolution of the diagnostic Raman peaks with the

temperature in methanol-saturated atmosphere that confirms the switching from HS to LS

state cooling the sample from room temperature to <255 K. It must be noted as in the case of

crystallites exposed to an ethanol atmosphere it was not possible to investigate the thermal

behaviour by Raman spectroscopy using our set-up because of the ethanol condensation

occurring on the sample surface during the cooling process. This condensation led to

D. Gentili et al. *J. Mater. Chem. C*

crystallites fully immersed in ethanol. In these conditions crystallites do not show the thermal transition (we tested starting from 170 K without observing any transition). On the other hand working under OM the measurements are much faster and can be performed limiting the ethanol condensation.
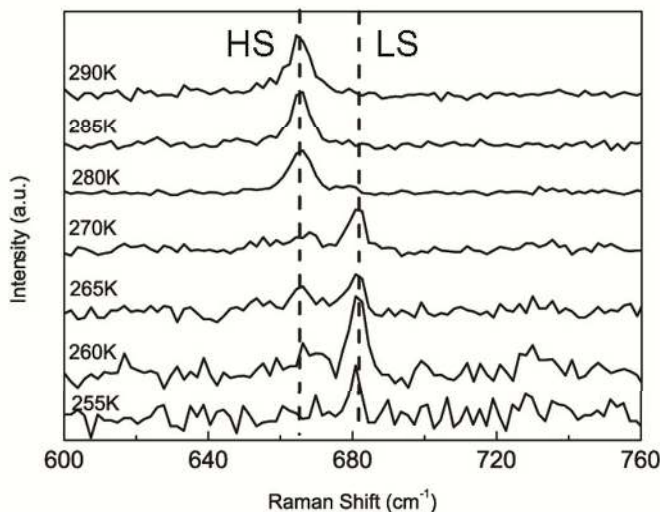
Figure 6. Temperature evolution of diagnostic Raman peak of **1** in saturated atmosphere of methanol vapour.

Structural investigation on compound **1** allowed to get atomic level details about the alcohol sensing phenomena. The X-ray diffraction has been conducted on selected, bigger crystals, which despite the small size were suitable for synchrotron X-ray diffraction analysis.

High quality diffraction data have been acquired for three different cases: dried crystals, crystals exposed to methanol and crystals exposed to ethanol. For each case temperature has been changed from 300K down to 100K using the same crystal (see detail of preparation in experimental section).

For dried crystals, the structural parameters obtained for the iron complex at both temperatures, are in agreement with data already published for compound **1**[27]. A different distribution of disordered solvent in cavities has been found and it has been interpreted with 1.25 water molecules in the asymmetric unit (ASU) (Figure 7a, 7d). The iron complex show a low spin configuration at both temperatures, as confirmed by the red crystal colour, the iron

Journal of Materials Chemistry C   **Page 12 of 26**

D. Gentili et al. *J. Mater. Chem. C*

coordination sphere bond lengths [27, 31, 32], the $N_{pyrazole}$–Fe–$N_{tetrazole}$ angles close to 160° (ca. 160° for LS and 145° for HS) and the Σ parameter close to 90° (ca. 90° for LS and 160° for HS)[33, 34] (Table 1).
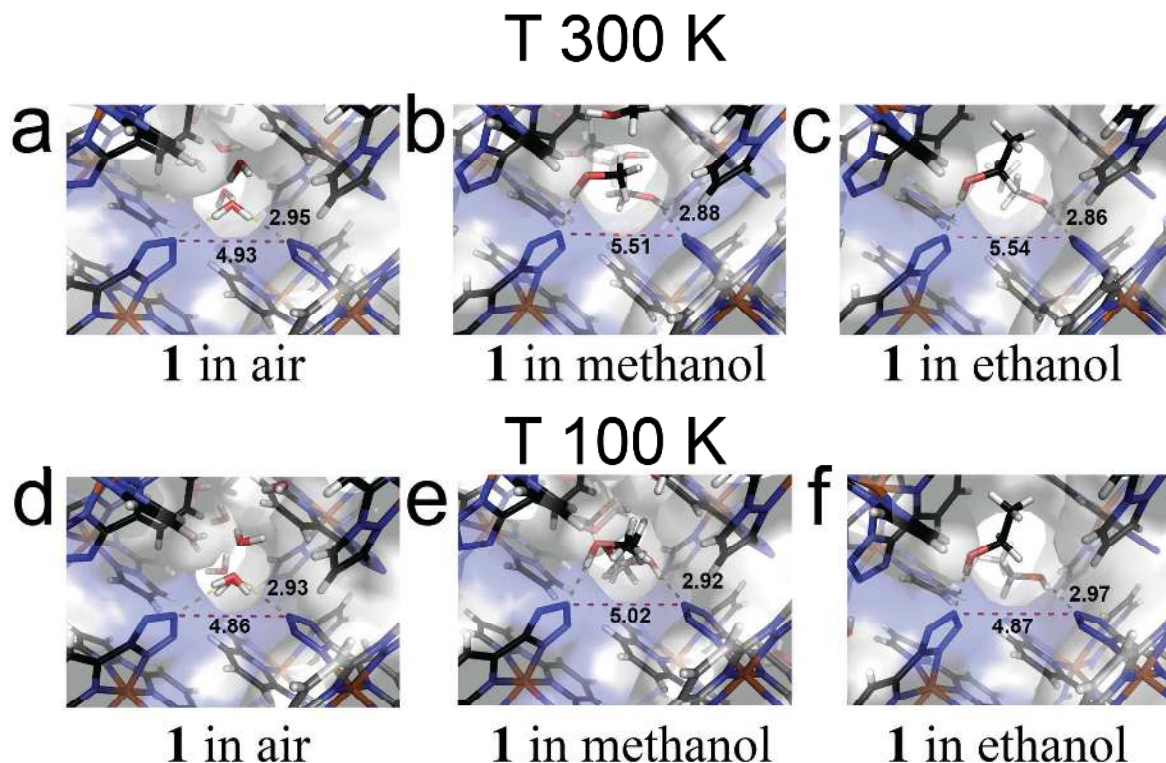
Figure 7. Partial view of crystal packing showing crystal cavity and solvent molecules in the ASU. Complex **1** molecules are represented with sticks (grey for ASU molecule and black for symmetry generated ones). a), b) and c) correspond to structures at 300K for dried crystals, methanol and ethanol exposed ones. d), e) and f) correspond to structures at 100K for dried crystals, methanol and ethanol exposed ones. Hydrogen bonds with tetrazole N10 are shown with yellow dashes, while N10-N10$_{sym}$ distance is represented with red dashes (Å).

D. Gentili et al. *J. Mater. Chem. C*

Table 1. Bond lengths (Å), significant angles (°) and naming scheme adopted for iron coordination sphere. The last line reports the distance between tetrazole nitrogen atom N10 of symmetry related molecules; this atom is in close contact with solvent molecules inside crystal cavities.

	Dried Crystals (published)	Dried Crystals	Dried Crystals	Crystals with Methanol	Crystals with Methanol	Crystals with Ethanol	Crystals with Ethanol
T (K)	180	300	100	300	100	300	100
Fe-N1	1.968(4)	1.978(1)	1.971(5)	2.198(1)	1.970(2)	2.201(2)	1.981(3)
Fe-N7	1.949(4)	1.962(1)	1.968(6)	2.213(1)	1.965(2)	2.210(3)	2.039(3)
Fe-N5	1.916(3)	1.912(1)	1.907(4)	2.144(2)	1.910(2)	2.146(4)	1.929(4)
Fe-N12	1.918(3)	1.912(1)	1.908(4)	2.152(2)	1.912(2)	2.156(5)	1.920(4)
Fe-N8	1.971(4)	1.980(1)	1.975(5)	2.162(1)	1.986(2)	2.159(3)	2.054(3)
Fe-N14	1.959(4)	1.971(1)	1.958(5)	2.204(1)	1.976(2)	2.207(2)	1.991(3)
N1-Fe-N7	160.04(14)	159.75(5)	160.02(19)	147.22(4)	159.91(6)	147.11(10)	159.31(13)
N14-Fe-N8	159.83(14)	159.86(5)	159.92(18)	147.20(5)	159.81(6)	146.77(10)	158.55(12)
Σ^*	87.2	88.6	87.6	148.5	87.5	149.7	105.7
Colour	Red	Red	Red	*Yellow*	Red	*Yellow*	Red
Spin Status	**LS**	**LS**	**LS**	***HS***	**LS**	***HS***	**LS**
N10-N10$_{sym}$	5.054(5)	4.932(2)	4.864(5)	5.506(5)	5.024(3)	5.540(10)	4.872(7)

$$^* \Sigma = \sum_{i=1}^{12} \left| \varphi_i - 90 \right|,$$ φ_i is an N–Fe–N octahedron angle with two N atoms in cis.
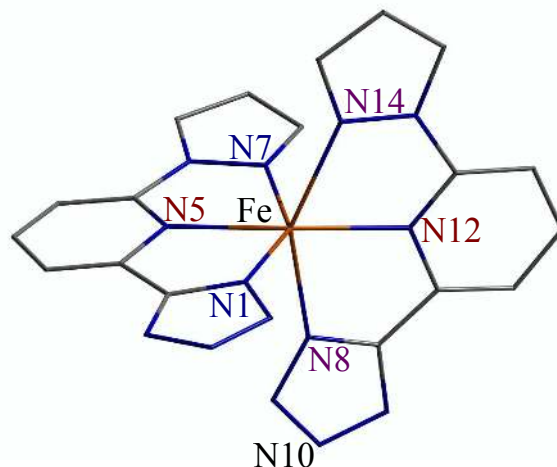
Exposure to methanol, converts the red dried crystals to a bright yellow form in a few seconds. The crystals obtained are very prone to switch back to the original red form as soon as the partial pressure of methanol decreases. Crystal exposed to the alcohol was quickly dipped in N-Paratone oil, which limits the methanol loss, and tested by diffraction.

Structural model obtained at 300K show a significant lengthening of all Fe-N bonds in metal coordination sphere in agreement with an high spin configuration of iron (Table 1 - N$_{pyrazole}$–Fe–N$_{tetrazole}$ $\cong$ 160° and $\Sigma \cong$ 160°).

The superimposition of the models with different iron spin configuration shows significant distortion also in the angle between the L$^-$ ligand molecules planes and the mean iron coordination planes (Figure 8).
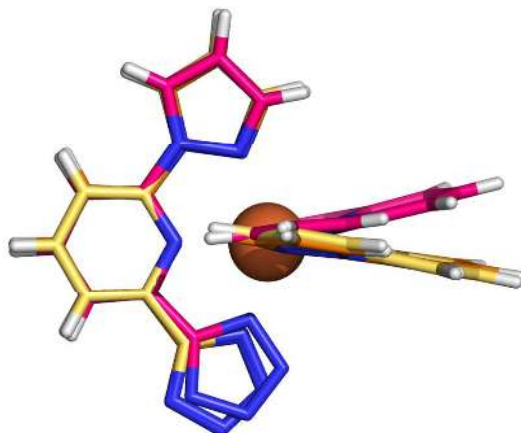
Figure 8. Superimposition of complex **1** in Low Spin (dried crystals at 300 K – hot pink sticks) and High Spin configurations (methanol exposed crystals at 300 K – orange sticks – and ethanol exposed crystals at the same temperature – yellow sticks).

Electron density in the voids shows the presence of methanol molecules; one of them, with full occupancy, is coordinated through hydrogen bond to N10 nitrogen of the tetrazole ring exposed to crystal cavities (Figure 7b and 7e).

The same crystal, cooled to 100K switches to the red LS state, with a structure equivalent to that of the dried crystal at this temperature.

In the case of exposure to ethanol, crystals of **1** exhibit a similar transition than in methanol but with much slower diffusion times and kinetics.

Crystalline model determined at 300K shows the structural descriptors of a high-spin iron complex with one fully occupied and well-ordered ethanol molecule in the ASU (Figure 9 and Figure 7c, 7f).

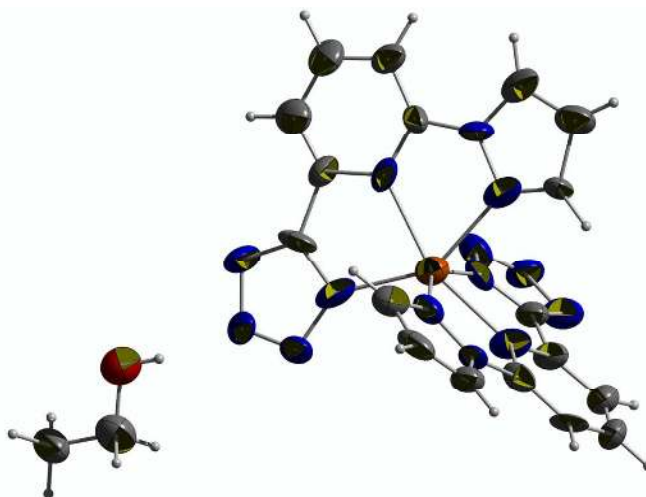D. Gentili et al. *J. Mater. Chem. C*

Figure 9. Asymmetric unit of **1,** crystals exposed to ethanol, obtained by X-ray diffraction at 100K. Displacement ellipsoids are drawn at 50% probability.

A LS state is reached cooling to 100K, with a slightly different configuration of the iron coordination sphere compared to the other dataset collected at 100K. This is probably associated to the increased solvent steric hindrance in the cavities: ethanol-containing voids are higher in this structure compared to methanol and dried ones (Table 2).

Table 2. Unit cell parameters, volumes and basic statistics for different crystals of molecule **1** collected.

	Dried Crystals (published)	Dried Crystals	Dried Crystals	Crystals with Methanol	Crystals with Methanol	Crystals with Ethanol	Crystals with Ethanol
T (K)	180(2)	300(2)	100(2)	300(2)	100(2)	300(2)	100(2)
a (Å)	23.896(6)	23.784(7)	23.709(1)	24.495(16)	23.843(5)	24.389(49)	23.815(29)
b (Å)	14.9259(19)	14.518(1)	14.472(2)	14.671(3)	14.824(3)	14.586(5)	14.299(5)
c (Å)	15.619(5)	15.534(2)	15.326(49)	16.712(9)	15.571(2)	16.985(21)	17.265(5)
β (°)	129.108(15)	127.854(5)	127.617(14)	131.374(24)	129.178(9)	131.227(38)	131.676(33)
V (Å^3)	4322.5(18)	4235.2(14)	4165(13)	4507(4)	4266.3(13)	4544(11)	4391(6)
Voids V (Å^3)*	663.7	562.5	552.3	763.2	638.8	813.0	704.4
Space Group	*C* 2/*c*	*C* 2/*c*	*C* 2/*c*	*C* 2/*c*	*C* 2/*c*	*C* 2/*c*	*C* 2/*c*
R1 [I>2σ(I)]	0.0495	0.0323	0.0756	0.0338	0.0458	0.0514	0.0596
Goof	0.847	1.049	1.110	1.046	1.079	1.030	1.059
Max Res. (Å)	0.85	0.72	0.74	0.74	0.72	0.72	0.74
Crystal colour	Red	Red	Red	Yellow	Red	Yellow	Red
Spin Status	**LS**	**LS**	**LS**	*HS*	**LS**	*HS*	**LS**
* Calculated with Platon VOID function [35]							

The Fe coordination bond lengths found are in agreement with other LS structures of published Fe[II] complexes bearing nitrogen containing ligands[31, 32].

After data collection at 100K all the crystals exposed to alcohol have been heated again up to room temperature recovering the original HS state preserving the methanol/ethanol in the cavities. As expected, the dried crystal remained red going back to 300K.

As shown in figure 7 in all the structures there is a solvent molecule coordinated to a ligand tetrazole ring exposed on crystal cavity. For dried crystals the N10 coordinated water **1** lies on a twofold axis and is bridging two neighbour complex molecules through hydrogen bonds. In presence of methanol and ethanol this H-bond crosslink is not possible and this introduces small local changes in the packing. This is in agreement with a ~4% volume increase and ~10% increase between $N10$-$N10_{sym}$ distance from low to high spin structures (Table 2).

Assuming that hydrogen bonds between N10 and different alcohols have similar strengths, this packing evidence suggests that the spin crossover phenomena could be mainly a lattice driven phenomena. The switch from high spin to low spin state seems triggered by bond contractions associated with temperature reduction, while solvent water replacement with bulkier molecules deform cavities and increase voids promoting high spin status. Dried crystals spin status switching to HS at temperature >300K is also consistent with this hypothesis assuming that water in channels is removed upon heating.

Complete diffraction data statistics, refinement protocols and further experimental details can be found in the supplementary materials.

Structural models have been deposited on The Cambridge Crystallographic Data Centre. Access codes are: CCDC-1055429 for molecules **1** in dried crystals (300K), CCDC-1055430 for dried crystals at 100K, CCDC-1055431 for crystals exposed to methanol at 300K, CCDC-1055432 for crystals exposed to methanol at 100K, CCDC-1055433 for crystals exposed to

D. Gentili et al. *J. Mater. Chem. C*

ethanol at 300K, CCDC-1055434 for crystals exposed to ethanol at 100K. These data can be

obtained free of charge via www.ccdc.cam.ac.uk/data_request/cif.

2.3. Multi-modal sensing

This behaviour prompts us to use **1** as multi-modal sensing material for methanol and ethanol.

For this purpose we used the same set-up already used for time temperature integrators TAG,

which are devices able to record their thermal history, by quantitative reading of the colour

evolution[36] or the birefringence[37] directly on micrometric TAGs[38].

With this purpose we deposited some crystallites of **1** on a pre-patterned surface. In

particular we patterned a TAG containing an Aztec code[36]. Patterning of the active material or

the pre-fabrication of some markers is necessary in order to make the crystallites addressable,

thus readable, by a CCD. Figure 10 shows an optical image of a crystallite deposited by

lithographically controlled wetting[39, 40] into a pre-patterned pixel of a TAG fabricated on
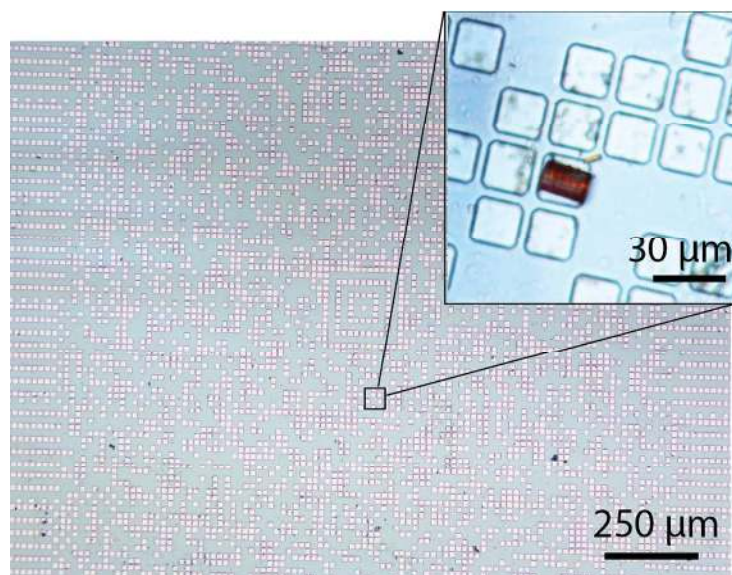
silicon surface.

Figure 10 Optical image of an addressable crystallites printed on a micrometric TAG. The position of the crystal is addressable by conventional readers for micro TAGs.

A commercial CCD is used to record the optical and cross-polarised images of specific crystallites both at room temperature and during the thermal treatment under alcohols atmosphere.

Figure 11 shows the number of counts of the red (R), green (G) and blue (B) component recorded by the CCD as a function of the temperature at which the device was exposed for 10 s; each image was recorded fixing the intensity of illumination and the time of acquisition of the CCD (see detail in the method section). The quantitative analysis of the optical images shows that for each temperature the colour recorded by the CCD is formed by a unique and defined combination of RGB components. The specific colour combination is an interpretation of the CCD, it depends on the particular CCD and illumination and therefore, in order to have a quantitative detection, each CCD must be calibrated. The RGB combination of each colour is itself a way to distinguish whether a crystal is exposed to the methanol or ethanol. However a further confirmation was obtained monitoring the thermal behaviour of crystallites.

In particular we recorded the composition of the colour upon the thermal treatment of **1.**

As shown in figure 11, while the red component shows a mean constant decreasing during the cooling, the CCD reads the spin transition as a strong change of the green component. The transition is evident as in the bright field images as in the crossed-polar images. It occurs at 270 ± 3 K and at 256 ± 3 K for crystal exposed to methanol and ethanol respectively. This difference led us to unambiguously discern between methanol and ethanol.
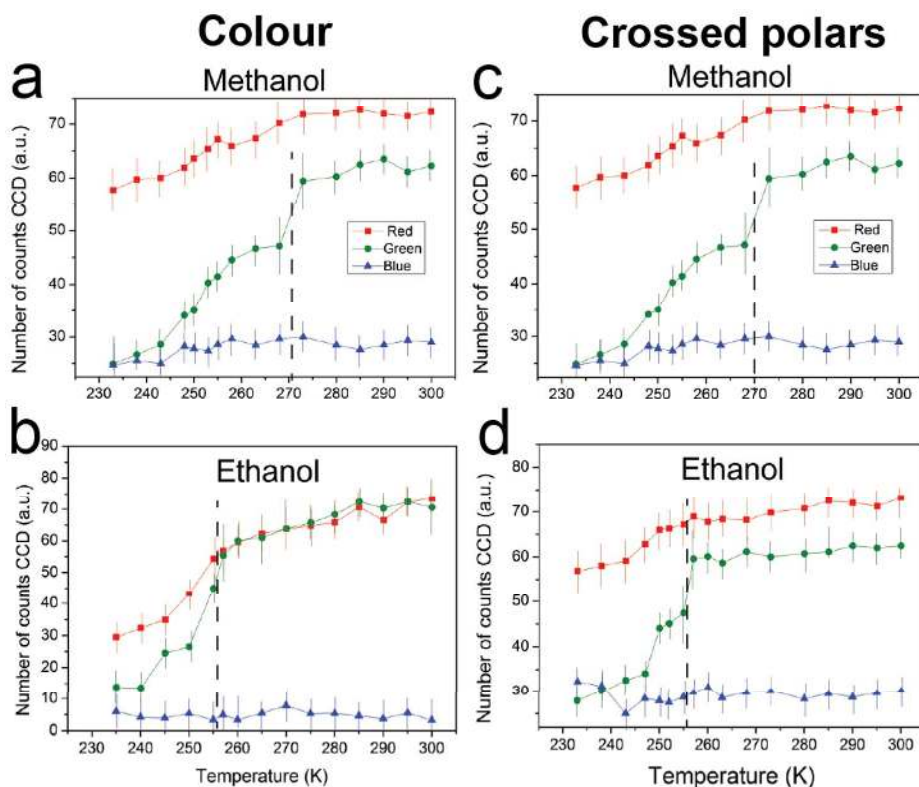
D. Gentili et al. *J. Mater. Chem. C*

Figure 11. Quantitative analysis of the optical images. A commercial CCD recorded optical images. The colours of the graphs correspond to the colours component of the CCD (red, blue, green). a) Number of counts versus temperature obtained for crystal of **1** exposed to saturate atmosphere of methanol b) Number of counts versus temperature obtained for a crystal of **1** exposed to saturate atmosphere of ethanol. Each image was recorded fixing the intensity of illumination and the time of acquisition of the CCD. c, d) Corresponding number of counts versus temperature obtained in cross polars images.

4. Experimental

4.1 Crystallization and alcohol sensing experiments setup.

Dried crystals of SCO complex **1**, methanol exposed crystals and ethanol exposed crystals, suitable for diffraction experiments, have been obtained from a $CH_3OH:CH_2Cl_2$ 1:1 solution by drop casting and slow evaporation (largest size 200 μm), at 4°C on Si wafers. Crystals with different habits can be obtained: some have an elongated parallelepiped shape; others appear as bright red blocks that grows in the three dimensions, with more homogeneous lengths. Alcohol interactions have been studied equilibrating the crystals at room temperature (300 K) in Petri dishes. Same results can be detected using vapours or dipping the crystals in the

Journal of Materials Chemistry C

Page 20 of 26

D. Gentili et al. *J. Mater. Chem. C*

liquid alcohol. To limit lattice stress connected to complete solvent removal (crystals dried out) and solvent reintroduction, part of the crystals have been kept in their mother liquors and transferred to methanol or ethanol, without letting them desolvate.

This approach is useful for methanol but it is not successful for ethanol: electron density maps, which can be obtained with this approach, still show the presence of methanol inside crystal channels (incorporated from the original mother liquors). This result suggested that proper ethanol sensing experiments had to be done on "activated" fully dried crystals.

Samples deposited on the surface were prepared following the procedures described in refs.[41, 42].

4.2 Optical microscopy

Optical micrographs were recorded with a Nikon i-80 microscope equipped with epi-illuminator and cross polars (POM). The images presented were recorded using objective: LU Plan ELWD 20X/0.40 and 50X/0.55 objectives. Images were recorded by a commercial CCD (DIGITAL SIGHT DS-2MV).

4.3 Raman spectroscopy

Nd-YAG excitation wavelength (532 nm) was used to obtain Raman spectra in the $100-2000$ cm^{-1} range. Raman scattering measurements were recorded in backscattering configuration using a long working-distance 50X microscope objective with laser power lower than 25 μW to avoid photo-thermal effects. The samples were mounted in a Liquid Nitrogen Peltier heating-cooling stage to span the 150 - 400 K temperature range.

4.4 Thermal treatment and temperature control

The thermal treatments were performed under the optical microscope using a heating stage Linkham TMHS600 connected to a TP94 controller, with a control of 0.1 °C using the setup described in ref. [43].

D. Gentili et al. *J. Mater. Chem. C*

4.5 X-ray diffraction data collections

Data collections were performed for all these systems at the X-ray diffraction beamline (XRD1) of the Elettra Synchrotron, Trieste (Italy) with a Pilatus 2M image plate detector. Complete datasets have been collected at a monochromatic wavelength of 0.700 Å through the rotating crystal method. Crystals of **1** and **1** exposed to alcohols, were dipped in N-paratone, to limit solvent exchange during data acquisitions, and mounted on the goniometer head with a nylon loop. The diffraction datasets were collected at controlled temperatures, using a nitrogen stream supplied through an Oxford Cryostream 700: for all the samples data collected at room temperature and 100K, from the same crystal are reported in this work. Significant changes have been detected for systems exposed to alcohols as a function of temperature. The diffraction data were indexed, integrated and scaled using XDS[44]. The structures were solved by direct methods using SIR-2014[45], Fourier analyzed and refined by the full-matrix least-squares based on F^2 implemented in SHELXL-2014[46]. Coot program has been used for modelling[47]. In the final refinement, all non-hydrogen atoms with full occupancy, were treated anisotropically and the hydrogen atoms were included at calculated positions with isotropic $U_{factors} = 1.2 \cdot U_{eq}$ or $U_{factors} = 1.5 \cdot U_{eq}$ for methyl groups.

Data from a bigger crystal of the dried form of **1** have been corrected for absorption as implemented in the XABS2 program[48].

5. Conclusions

In conclusion we report on the characterization of a neutral SCO able to switch around room temperature. We proved that compound **1** can be used as high-selective material for sensing of methanol and ethanol by a multi-modal response. We showed that in correspondence of the spin transition **1** exhibits a simultaneous change of colour, birefringence and Raman spectra, which we exploited in a multi-modal sensor. The transition temperature dramatically

changes when **1** is exposed to methanol or ethanol. Structural details of alcohols adsorption in the crystals and spin transition have been successfully followed exploiting X-Ray diffraction and interpreted at atomic scale. We proved that comparing the colours components and the thermal behaviour, we can efficiently distinguish when a crystallite deposited on a patterned surface was exposed to methanol or ethanol, demonstrating it direct application in TAG sensors.

Despite the facts that the switch of colour and birefringence are particularly intense for compound **1**, they are well-known and common in SCO compounds; this fact allow us to be confident that similar approach can be extended to many other SCO compounds, enabling new applicative perspective for this class of materials.

7. Acknowledgements

D. Gentili et al. *J. Mater. Chem. C*

8. Bibliographic references and notes

1.   O. Kahn and C. J. Martinez, *Science*, 1998, 279, 44-48.

2.   E. Breuning, M. Ruben, J. M. Lehn, F. Renz, Y. Garcia, V. Ksenofontov, P. Gutlich, E. Wegelius and K. Rissanen, *Angew. Chem., Int. Ed.*, 2000, 39, 2504.

3.   P. Gutlich, Y. Garcia and H. A. Goodwin, *Chem. Soc. Rev.*, 2000, 29, 419-427.

4.   O. Sato, *Acc. Chem. Res.*, 2003, 36, 692-700.

5.   S. Bonhommeau, T. Guillon, L. M. L. Daku, P. Demont, J. S. Costa, J. F. Letard, G. Molnar and A. Bousseksou, *Angew. Chem., Int. Ed.*, 2006, 45, 1625-1629.

6.   A. Bousseksou, G. Molnar, P. Demont and J. Menegotto, *J. Mater. Chem.*, 2003, 13, 2069-2071.

7.   F. Varret, K. Boukheddaden, E. Codjovi and A. Goujon, *Hyperfine Interact.*, 2005, 165, 37-47.

8.   M. Cavallini, *Phys. Chem. Chem. Phys.*, 2012, 14, 11867-11876.

9.   M. Cavallini, I. Bergenti, S. Milita, J. C. Kengne, D. Gentili, G. Ruani, I. Salitros, V. Meded and M. Ruben, *Langmuir*, 2011, 27, 4076-4081.

10.   E. Coronado, C. Marti-Gastaldo, J. R. Galan-Mascaros and M. Cavallini, *J. Am. Chem. Soc.*, 2010, 132, 5456-5468.

11.   P. Gutlich, A. Hauser and H. Spiering, *Angew. Chem. Int. Ed.*, 1994, 33, 2024-2054.

12.   A. B. Gaspar and M. Seredyuk, *Coord. Chem. Rev.*, 2014, 268, 41-58.

13.   M. A. Halcrow, *Chem. Soc. Rev.*, 2011, 40, 4119-4142.

14.   M. A. Halcrow, *Chem. Lett.*, 2014, 43, 1178-1188.

15.   M. Nihei, T. Shiga, Y. Maeda and H. Oshio, *Coord. Chem. Rev.*, 2007, 251, 2606-2621.

16.   A. Bousseksou, G. Molnar, L. Salmon and W. Nicolazzi, *Chem. Soc. Rev.*, 2011, 40, 3313-3335.

17.   M. C. Young, E. Liew and R. J. Hooley, *Chem. Commun.*, 2014, 50, 5043-5045.

18.   M. Bartel, A. Absmeier, G. N. L. Jameson, F. Werner, K. Kato, M. Takata, R. Boca, M. Hasegawa, K. Mereiter, A. Caneschi and W. Linert, *Inorg. Chem.*, 2007, 46, 4220-4229.

D. Gentili et al. *J. Mater. Chem. C*

19. H. L. C. Feltham, C. Johnson, A. B. S. Elliott, K. C. Gordon, M. Albrecht and S. Brooker, *Inorg. Chem.*, 2015, 54, 2902-2909.

20. F. Prins, M. Monrabal-Capilla, E. A. Osorio, E. Coronado and H. S. J. van der Zant, *Adv. Mater.*, 2011, 23, 1545-1549.

21. M. Cavallini, I. Bergenti, S. Milita, G. Ruani, I. Salitros, Z. R. Qu, R. Chandrasekar and M. Ruben, *Angew. Chem.-In. Ed.*, 2008, 47, 8596-8600.

22. V. Meded, A. Bagrets, K. Fink, R. Chandrasekar, M. Ruben, F. Evers, A. Bernand-Mantel, J. S. Seldenthuis, A. Beukman and H. S. J. van der Zant, *Phys. Rev. B*, 2011, 83.

23. A. D. Naik, K. Robeyns, C. F. Meunier, A. F. Leonard, A. Rotaru, B. Tinant, Y. Filinchuk, B. L. Su and Y. Garcia, *Inorg. Chem.*, 2014, 53, 1263-1265.

24. J. Linares, E. Codjovi and Y. Garcia, *Sensors*, 2012, 12, 4479-4492.

25. Y. S. Koo and J. R. Galan-Mascaros, *Adv. Mater.*, 2014, 26, 6785-6789.

26. C. Bartual-Murgui, A. Akou, C. Thibault, G. Molnar, C. Vieu, L. Salmon and A. Bousseksou, *J. Mater. Chem. C*, 2015, 3, 1277-1285.

27. B. Schafer, C. Rajnak, I. Salitros, O. Fuhr, D. Klar, C. Schmitz-Antoniak, E. Weschke, H. Wende and M. Ruben, *Chem. Commun.*, 2013, 49, 10986-10988.

28. We identified a minor impurity of a few crystallites (<5%), which contain an excess of ligand in the crystal structure. These crystals donot exhibit the spin transition in the range of temperature 170-320 K (above 320 K they decompose)

29. G. Brehm, M. Reiher, B. Le Guennic, M. Leibold, S. Schindler, F. W. Heinemann and S. Schneider, *J. Raman Spectrosc.*, 2006, 37, 108-122.

30. D. Maspoch, D. Ruiz-Molina, K. Wurst, N. Domingo, M. Cavallini, F. Biscarini, J. Tejada, C. Rovira and J. Veciana, *Nat. Mater.*, 2003, 2, 190-195.

31. C. Genre, G. S. Matouzenko, E. Jeanneau and D. Luneau, *New J. Chem.*, 2006, 30, 1669-1674.

32. A. Kaiba, H. J. Shepherd, D. Fedaoui, P. Rosa, A. E. Goeta, N. Rebbani, J. F. Letard and P. Guionneau, *Dalton Trans.*, 2010, 39, 2910-2918.

33. I. Salitros, O. Fuhr, R. Kruk, J. Pavlik, L. Pogany, B. Schafer, M. Tatarko, R. Boca, W. Linert and M. Ruben, *Eur. J. Inorg. Chem.*, 2013, DOI: 10.1002/ejic.201201123, 1049-1057.

D. Gentili et al. *J. Mater. Chem. C*

34.   I. Salitros, J. Pavlik, R. Boca, O. Fuhr, C. Rajadurai and M. Ruben, *CrystEngComm*, 2010, 12, 2361-2368.

35.   A. L. Spek, *J. Appl. Crystallogr.*, 2003, 36, 7-13.

36.   D. Gentili, M. Durso, C. Bettini, I. Manet, M. Gazzano, R. Capelli, M. Muccini, M. Melucci and M. Cavallini, *Sci. Rep.*, 2013, 3, 2581.

37.   M. Cavallini, A. Calo, P. Stoliar, J. C. Kengne, S. Martins, F. C. Matacotta, F. Quist, G. Gbabode, N. Dumont, Y. H. Geerts and F. Biscarini, *Adv. Mater.*, 2009, 21, 4688-4691.

38.   D. Gentili, M. Barbalinardo, I. Manet, M. Durso, M. Brucale, A. Mezzi, M. Melucci and M. Cavallini, *Nanoscale*, 2015, 7, 7184-7188.

39.   M. Cavallini, D. Gentili, P. Greco, F. Valle and F. Biscarini, *Nat. Protoc.*, 2012, 7, 1668-1676.

40.   M. Cavallini, M. Facchini, M. Massi and F. Biscarini, *Synth. Met.*, 2004, 146, 283-286.

41.   M. Cavallini, R. Lazzaroni, R. Zamboni, F. Biscarini, D. Timpel, F. Zerbetto, G. J. Clarkson and D. A. Leigh, *J. Phys. Chem. B*, 2001, 105, 10826-10830.

42.   P. Leclere, M. Surin, R. Lazzaroni, A. F. M. Kilbinger, O. Henze, P. Jonkheijm, F. Biscarini, M. Cavallini, W. J. Feast, E. W. Meijer and A. Schenning, *J. Mater. Chem.*, 2004, 14, 1959-1963.

43.   A. Calo, P. Stoliar, M. Cavallini, Y. H. Geerts and F. Biscarini, *Rev. Sci. Instrum.*, 2010, 81.

44.   W. Kabsch, *Acta Crystallogr., Sect. D: Biol. Crystallogr. y*, 2010, 66, 125-132.

45.   M. C. Burla, R. Caliandro, M. Camalli, B. Carrozzini, G. L. Cascarano, C. Giacovazzo, M. Mallamo, A. Mazzone, G. Polidori and R. Spagna, *J. Appl. Crystallogr.*, 2012, 45, 357-361.

46.   G. M. Sheldrick, *Acta Crystallogr., Sect. A: Found. Adv.*, 2008, 64, 112-122.

47.   P. Emsley and K. Cowtan, *Acta Crystallogr., Sect. D: Biol. Crystallogr.*, 2004, 60, 2126-2132.

48.   S. Parkin, B. Moezzi and H. Hope, *J. Appl. Crystallogr.*, 1995, 28, 53-56.

Tables of contents entry

We demonstrate multi-modal sensing capabilities to short chain alcohols of spin crossover compounds by integrating them in a micrometric TAG sensible to the colour and birefringence.